2021 43rd Annual International Conference of the
IEEE Engineering in Medicine & Biology Society (EMBC)
Oct 31 - Nov 4, 2021. Virtual Conference

A Multiplexed Microfluidic Device to Measure Blood-Brain Barrier Disruption by Pulsed Electric Fields

Philip M. Graybill and Rafael V. Davalos, *Member, IEEE*

Abstract— **Local disruption of the blood-brain barrier (BBB) by pulsed electric fields shows significant potential for treating neurological conditions. Microfluidic BBB models can provide low-cost, controlled experiments with human cells and test a range of parameters for preclinical studies. We developed a multiplexed BBB device that can test a three-fold range of electric field magnitudes. A tapered channel creates a linear gradient of the electric field within the device, and an asymmetric branching channel enables an on-chip control. We monitored BBB permeability in real-time using the diffusion of a fluorescent marker across an endothelial monolayer to determine BBB disruption after high-frequency bipolar electrical pulses (HFIRE). We show that HFIRE pulses can transiently open the BBB. Unexpectedly, electrofusion of cells resulted in decreased permeability for some conditions. Our multiplexed device can efficiently probe treatment variables for efficient preclinical testing of optimal parameters for reversible BBB disruption.**

Clinical Relevance—**This *in vitro* model of the BBB can inform preclinical studies by investigating a range of electroporation parameters for BBB disruption.**

I. Introduction

Despite decades of research, many neurological diseases and disorders remain challenging to treat. For example, glioblastoma, an aggressive brain cancer, is almost universally fatal within 1-2 years.[1] Parkinson's disease and Alzheimer's disease are rapidly increasing in prevalence worldwide with no cure.[2, 3] Treatment of these conditions and other neurological diseases and disorders is hampered by the protective nature of the blood-brain barrier (BBB). The BBB is composed of specialized endothelial cells surrounded by supporting cells such as astrocytes and pericytes, and restricts transport between the blood and the brain tissue to maintain a neuro-protective microenvironment.[4] The BBB is a severe blockade to effective therapy of neurological diseases. Nearly 100% of all large-molecule drugs and ~98% of small-molecule drugs cannot penetrate the BBB.[5]

Recent *in vivo* and *in vitro* research has demonstrated that high voltage pulsed electric fields (PEFs) are able to transiently disrupt the BBB.[6-9] PEFs cause unregulated transmembrane molecular diffusion through the creation of membrane pores, an effect known as electroporation. [10] In a recent paper, we have demonstrated that 100 µs pulsed electric fields can increase the permeability of an endothelial monolayer.[6] Here, we improve our design for increased throughput: a tapered channel creates an electric field gradient in the device that enables six electric fields to be investigated simultaneously on the same chip. Furthermore, we investigate BBB disruption following high-frequency irreversible electroporation (HFIRE) waveforms comprised of 2-µs bipolar pulses. Microfluidic *in vitro* BBB models provide an excellent method for exploration of the vast parameter space of HFIRE therapies, and our multiplexed device can further enhance efficiency. *In vivo* studies are limited by high costs, labor-intensive experiments, confounding variables, and species-specific responses. Microfluidic *in vitro* models, however, can overcome these limitations to provide low-cost, high-throughput, well-controlled experiments using human cell types.

Our results demonstrate that our multiplexed device is able to measure the responses of the BBB to various electric field magnitudes simultaneously, while controlling for undesired experimental variability with an on-chip control. Using our device, we show that 2 µs bipolar HFIRE pulses transiently increase BBB permeability in the first 30-60 minutes, and that BBB disruption is both field and burst-number dependent. Unexpectedly we found that some pulsing conditions reduced BBB permeability below pre-electroporation values following the transient increase in permeability.

II. Materials and Methods

A. Device Design and Fabrication

A simple geometry, illustrated in Figure 1, enables multiple electric field magnitudes to be tested in a single experiment. The microfluidic device is fabricated from two polydimethylsiloxane (PDMS) channel layers: an upper, tapered channel (red in Figure 1) and a bottom, branching channel. The two channel layers are separated at their intersections by a polyester track-etched membrane (0.4 µm pores). Devices are assembled as described previously.[6] Human cerebral microcapillary endothelial cells (hCMECs) are cultured within the tapered channel on the upper side of the permeable membrane to form a confluent monolayer. During an experiment, a fluorescent dye is introduced to the upper channel, and the diffusion of this tracer across the monolayer is measured in the bottom branching channels downstream of the intersection points. HFIRE pulses are applied to the device with acupuncture electrodes, one located at the wide end of the tapered channel and another located between the branched channels of the bottom layer.

Research supported by the NIH (P01CA207206).

R. V. Davalos is a professor at the Virginia Tech-Wake Forest School of Biomedical Engineering and Sciences, Blacksburg, VA 24060. (phone: (540) 231-1979; fax: 540-231-0970; e-mail: davalosr@vt.edu).

P. M. Graybill is a doctorate candidate at Virginia Tech, Blacksburg, VA, 24061 USA (pmg1@vt.edu).

The bottom channel branches from a single inlet into eight channels (0.1 x 0.8 x 8 mm), as shown in Figure 2a. The branching design creates eight intersection points with the top channel, enabling eight independent measurements of BBB permeability. Two control channels (leftmost channels in Figure 2a) are offset from the six treated channels. The flow rates in the branching network were equalized by adjusting the position of the inlet branching point to equalize the hydraulic resistance. COMSOL simulations indicate that the flow rate differs less than 0.1% between the eight channels despite the asymmetry (Figure 2a).

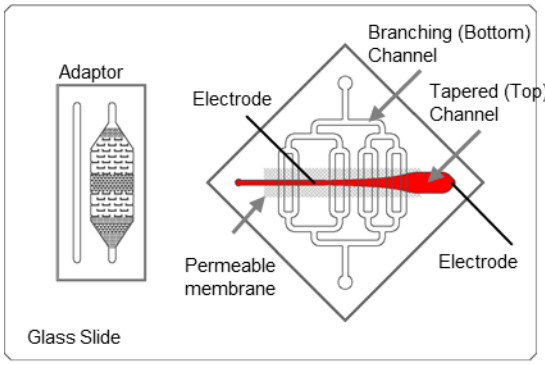

Figure 1. A schematic of the multiplexed BBB device.

The top channel has a specific tapered profile to produce a linear gradient of electric field, thereby enabling six electric field magnitudes to be tested over a three-fold range in a single experiment. The electric field in the channel is inversely related to the cross-sectional channel area according to Ohm's law:

$$\mathrm{E}(x) = \frac{1}{\sigma}\mathrm{J}(x) \sim \frac{1}{\sigma \mathrm{A(x)}} \quad (1)$$

where $E(x)$ is the electric field, σ is the conductivity of the medium, $\mathrm{J}(x)$ is the current density, and A(x) is the cross-sectional area of the channel.[11] Low-conductivity media in the lower branching channels confines electrical current to the top tapered channel. Using Equation 1, we created a 10-mm long tapered region with a width ranging from 0.75 mm to 2.25 mm to create a 3-fold range of electric fields. The tapered channel height is 250 µm. A COMSOL model of the electric field in the tapered channel indicates that a linear gradient of electric field magnitude is established within the tapered region (Figure 2b).

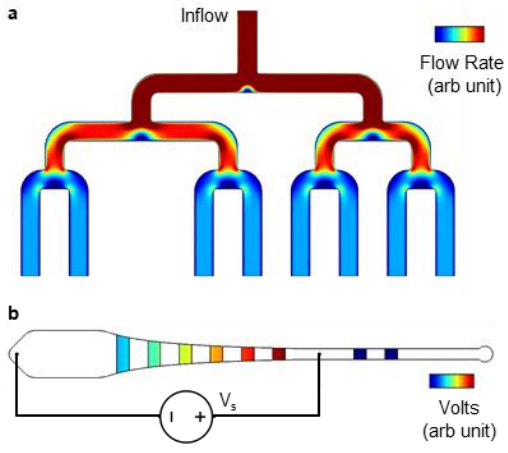

Figure 2. Finite element modeling of the device. a) Flow rates are balanced between the branching channels despite the asymmetry. b) The taper creates a linear gradient of electric field that spans a 3-fold range.

B. Permeability Measurement in the Device

Permeability is measured in real-time via the diffusion of fluorescein sodium salt (367 Da) across the endothelial monolayer from the top channel to the bottom channels (Figure 1c). During experiments, the fluorescent intensity of the eight lower channels were measured every 30 seconds by imaging downstream of the intersection points. Permeability of the system (membrane and monolayer) is calculated as described previously as:

$$P = \frac{U}{A}\left(\frac{I_F}{I_{F_0}}\right) \quad (2)$$

where P is the permeability [cm/s], U is the flow rate of the branching channel [cm^3/s], A is the intersection area [cm^2], I_F is the fluorescence intensity measured at the outlet, and I_{F_0} is the baseline intensity of the fluorescein media in the top channel.[6] Monolayer permeability is calculated by accounting for the permeability of the track-etched membrane.

Permeability measurements in our experiments are very sensitive, and monolayer permeability can change during experiments due to experimental conditions. Using the permeabilities measured in the control channels, we normalized the permeability data from the six test channels, as shown in Figure 3. As this figure demonstrates, the normalized data significantly reduces noise.

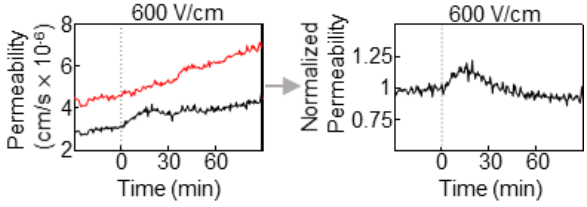

Figure 3. Control channel data (left, red) can be used to isolate permeability changes due to electroporation from the treated channels (left, black).

C. HFIRE Parameters

To validate this device, we treated the monolayer with HFIRE pulses and measured the permeability of the monolayer following treatment. Table 1 presents the HFIRE parameters tested. HFIRE pulses were delivered by a pulse generator as bursts of bipolar pulses: a 2-µs positive polarity pulse, followed by a 5-µs delay, followed by a 2-µs negative polarity pulse (2-5-2 µs waveform). Twenty-five 2-5-2 µs bipolar pulses were applied in series to achieve 100 µs total on-time to make a complete 'burst'. Bursts were delivered at 1 Hz, and burst number was varied from 10 to 200. Prior to administering the HFIRE pulses, permeability was monitored for 30 minutes to collect a baseline measurement. Experimental results were analyzed using Image-J. After the pulse administration, the permeability was monitored for 1.5 hours to capture permeabilization and recovery of the BBB.

Applied Voltage (V)	Burst Number	Electric Fields Tested
1034	10, 100	300, 420, 540, 660, 780, 900
3102	20, 200	900, 1260, 1620, 1980, 2340, 2700

D. Experimental Setup

Experiments were performed as described previously.[6] Syringe pumps provided fluid flow in the upper and lower channels. The tapered channel was perfused with complete media with 167 μg/ml of fluorescein sodium salt and the bottom channel was perfused with a low-conductivity buffer.

E. Cell Culture

Human cerebral microcapillary endothelial cells (hCMECs) were cultured using standard procedures in EndoGRO-MV complete media.

To seed the devices, the chips were sterilized with 70% ethanol, washed with PBS, and filled with 50 μg ml^{-1} human fibronectin in PBS and incubated for 1 hour at 37 °C. After incubation, the PBS was replaced with complete media and incubated for an additional hour. hCMECs were then seeded at a density of 10 million cells/ml and cultured in static conditions for 2 days to form confluent monolayers. Experiments were performed in a stage-top incubator at 5% CO_2. Post-experiment live-dead staining was performed using Calcein-AM and Propidium Iodide (PI).

III. Results

A. BBB Disruption after HFIRE

We applied 1034 V to the device to investigate cell response at 300, 420, 540, 660, 780, and 900 V/cm (Figure 4). Our results showed that BBB disruption was electric field magnitude and pulse number dependent. For 10 bursts, BBB disruption was minimal at 540 V/cm, moderate at 660 V/cm, and significant at 780 and 900 V/cm. Maximal disruption was reached approximately 15 minutes after electroporation, with permeabilities returning to near baseline by about 40 minutes. For 100 bursts, similar trends were observed.

We then applied 3102 V to the device to create electric fields of 900, 1260, 1620, 1980, 2340, and 2700 V/cm within the device, and investigated treatments of 20 and 200 HFIRE bursts. At 1620 V/cm and above, 200 HFIRE bursts resulted in a permanent increase in permeability. For 200 bursts at 900 and 1260 V/cm, however, we found a significant increase in membrane permeability during the first 60 minutes after electroporation. Treatment with 20 bursts at these electric fields resulted in unexpected permeability trends. Electroporation with 20 bursts at 900 V/cm yielded a transitory increase in monolayer permeability followed by a return to baseline values. Higher voltages from 1260 to 1980 V/cm, however, resulted in a minimal increase in permeability followed by a significant decrease in permeability. Likewise, at 2340 and 2700 V/cm a period of increased membrane permeability is followed by a period of significantly decreasing permeability.

A. Cell Viability and Morphology

Post-experiment staining showed high cell viabilities at lower voltages (300-900 V/cm), indicating the reversible nature of BBB disruption. This finding agrees with our permeability results, which demonstrated that permeability returned to baseline values after treatment. However, higher voltages (1620 – 2700 V/cm) for high burst numbers (200) show significant cell death that corresponds to irreversible BBB disruption. Interestingly, at high voltages (1260 – 2700 V/cm) and low burst number (20 bursts) cells show intact membranes (positive for Calcein AM but negative for PI) but a closer examination reveals significant amounts of electrofusion. Adjacent cells appear to be fused together. This finding suggests that the unexpected decrease in monolayer permeability after these treatment conditions resulted from significant electrofusion that reduced transport pathways between cells.

IV. Discussion

Our results demonstrate that our multiplexed microfluidic BBB device can simultaneously deliver electric pulses over a

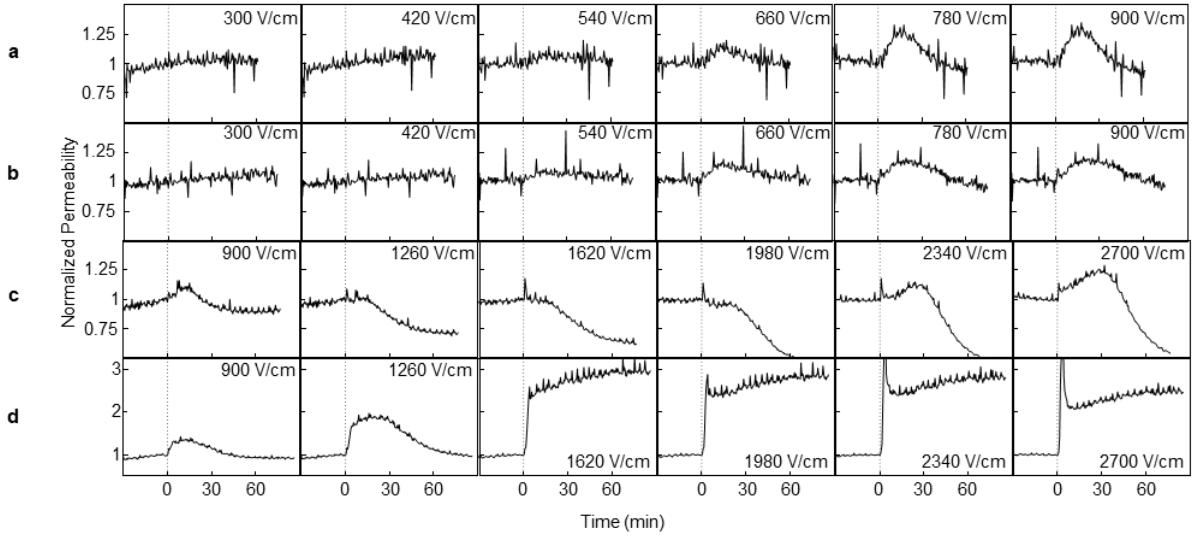

Figure 4. BBB disruption due to HFIRE treatment at lower voltages (300-900 V/cm, (a) 10 or (b) 100 bursts) and higher voltages (900-2700 V/cm, (c) 20 or (d) 200 bursts).

three-fold range of magnitudes, and measure membrane permeability of the treated endothelial monolayer in real-time. The normalization of permeability data by the on-chip control channels eliminated most unwanted noise due to flow rate changes, temperature changes, or changes in endothelial behavior due to experimental conditions (fluid flow, media, fluorescent dye, etc).

Our BBB permeability measurements for electric fields between 300 and 2700 V/ cm and for 10 to 200 HFIRE bursts, reveal electric field and pulse number dependent trends. Reversible electroporation at lower fields (300-900 V/cm) leads to a transitory increase in monolayer permeability in the first 30 to 60 minutes after treatment, followed by a recovery to pre-pulse permeability. Fields less than 900 V/cm resulted in high cell viability post-electroporation. Interestingly, electroporation with higher fields and low pulse number resulted in a transitory increase in permeability that was followed a decrease in permeability significantly below pre-electroporation levels. The decrease in permeability is likely due to electrofusion between adjacent cells, thus limiting paracellular transport of the fluorescent marker. Future studies should be conducted to determine if electrofusion occurs *in vivo* for these pulsing conditions. High voltages and high pulse number induced cell death and irreversible increases in monolayer permeability.

The results of this study were limited to 90 minutes post-electroporation, but significant endothelial recovery occurred during this timeframe. Recent *in vivo* results suggest that HFIRE may induce BBB disruption for up to 72 hours after treatment.[7] The short-term recovery seen in our experiments suggest that the prolonged BBB disruption *in vivo* is due to factors not replicated by our device. Possible sources of prolonged BBB disruption *in vivo* include pH changes, reactive oxygen species generation, immune activation, or interactions between endothelial cells and other cell types. I*n vitro* models with greater physiological relevance may help explain the prolonged disruption seen *in vivo.*

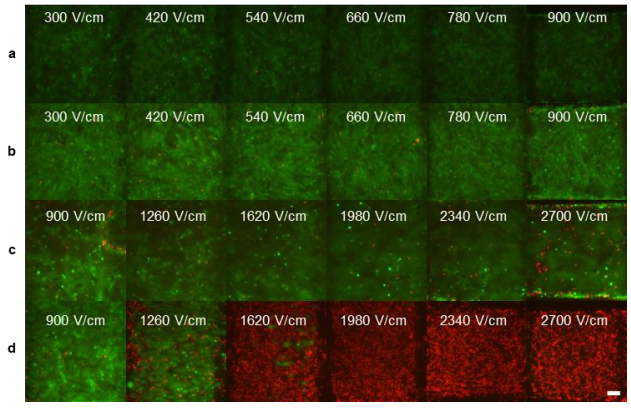

Figure 5. Viability analysis post HFIRE treatment for (a) 10 (b) 100 (c) 20 (d) 200 pulses. High viability is maintained at low voltages, but cell death and electrofusion occur at higher voltages. Scale bar 100 µm.

Our study used bi-polar HFIRE bursts, but our device could be used to study other types of electromagnetic stimuli including nanosecond pulses, microsecond pulses, and deep-brain stimulation waveforms.

V. Conclusion

Our microfluidic device can increase the efficiency of traditional microfluidic BBB experiments by providing six measurements of BBB permeability simultaneously. Furthermore, an on-chip control enables comparison with treated monolayers and can be used to remove unwanted noise by normalizing the data. We measured the permeability of an endothelial monolayer in real-time after HFIRE treatment. We show that BBB permeability can be increased by HFIRE pulses reversibly or irreversibly. Some pulsing conditions led to significant electrofusion and a subsequent decrease in permeability after treatment. Our device could be used to understand BBB responses to a variety of electroporation parameters prior to clinical translation for treatment of neurological diseases.

Acknowledgment

The authors thank Mohammad Bonakdar for guidance on this study.

References

References

[1] R. Stupp *et al.*, "Radiotherapy plus concomitant and adjuvant temozolomide for glioblastoma," (in English), *N. Engl. J. Med.,* Article vol. 352, no. 10, pp. 987-996, Mar 2005, doi: 10.1056/NEJMoa043330.

[2] E. R. Dorsey *et al.*, "Projected number of people with Parkinson disease in the most populous nations, 2005 through 2030," *Neurology,* vol. 68, no. 5, pp. 384-386, Jan 2007, doi: 10.1212/01.wnl.0000247740.47667.03.

[3] M. J. Prince, *World Alzheimer Report 2015: the global impact of dementia: an analysis of prevalence, incidence, cost and trends*. Alzheimer's Disease International, 2015.

[4] N. J. Abbott, A. A. K. Patabendige, D. E. M. Dolman, S. R. Yusof, and D. J. Begley, "Structure and function of the blood-brain barrier," *Neurobiology of Disease,* vol. 37, no. 1, pp. 13-25, Jan 2010, doi: 10.1016/j.nbd.2009.07.030.

[5] W. M. Pardridge, "Blood–brain barrier delivery," *Drug discovery today,* vol. 12, no. 1-2, pp. 54-61, 2007.

[6] M. Bonakdar, P. M. Graybill, and R. V. Davalos, "A microfluidic model of the blood-brain barrier to study permeabilization by pulsed electric fields," (in English), *Rsc Adv,* vol. 7, no. 68, pp. 42811-42818, 2017, doi: 10.1039/C7RA07603G.

[7] M. F. Lorenzo *et al.*, "Temporal Characterization of Blood–Brain Barrier Disruption with High-Frequency Electroporation," *Cancers,* vol. 11, no. 12, p. 1850, 2019.

[8] S. Sharabi *et al.*, "Transient blood–brain barrier disruption is induced by low pulsed electrical fields in vitro: an analysis of permeability and trans-endothelial electric resistivity," *Drug delivery,* vol. 26, no. 1, pp. 459-469, 2019.

[9] M. Hjouj *et al.*, "MRI Study on Reversible and Irreversible Electroporation Induced Blood Brain Barrier Disruption," *Plos One,* vol. 7, no. 8, Aug 2012, Art no. e42817, doi: 10.1371/journal.pone.0042817.

[10] J. C. Weaver and Y. A. Chizmadzhev, "Theory of electroporation: a review," *Bioelectrochemistry and bioenergetics,* vol. 41, no. 2, pp. 135-160, 1996.

[11] M. Bonakdar, E. M. Wasson, Y. W. Lee, and R. V. Davalos, "Electroporation of Brain Endothelial Cells on Chip toward Permeabilizing the Blood-Brain Barrier," *Biophysical journal,* vol. 110, no. 2, pp. 503-513, 2016.